Morphological Sharpening and Denoising Using a Novel Shock Filter Model

Cosmin Ludusan[1,2], Olivier Lavialle[2], Romulus Terebes[1], and Monica Borda[1]

[1] Technical University of Cluj-Napoca, 15 C. Daicoviciu Street, 400020, Cluj-Napoca, Romania
[2] Bordeaux 1 University, 351 Cours de la Libération, 33405, Talence, France
{Cosmin.Ludusan,Romulus.Terebes,Monica.Borda}@com.utcluj.ro,
Cosmin.Ludusan@etu.u-bordeaux1.fr,
Olivier.Lavialle@ims-bordeaux.fr

Abstract. We present a new approach based on Partial Differential Equations (PDEs) for image enhancement in generalized "Gaussian Blur (GB) + Additive White Gaussian Noise (AWGN)" scenarios. The inability of the classic shock filter to successfully process noisy images is overcome by the introduction of a complex shock filter framework. Furthermore, the proposed method allows for better control and anisotropic, contour-driven, shock filtering via its control functions f_1 and f_2. The main advantages of our method consist in the ability of successfully enhancing GB+AWGN images while preserving a stable-convergent time behavior.

Keywords: PDEs, shock filters, image denoising, image sharpening, image enhancement.

1 Introduction

The reasoning behind our approach has as starting point the limitations presented by the classic shock filter model described in [1] as well as on its subsequent developments, such as the one presented in [5]. The main drawback of the classic model consists in the fact that in the presence of AWGN the filtering is minimal, at best. This minimal filtering effect is mainly due to the numerical scheme based on the *minmod* function defined in [1] and used in computing the gradient norm in each point of the image function. Its role is to restrict large value variations in neighboring pixels, such being the case of noise-corrupted images. Another important drawback of the classic shock filter model resides in its edge detector, based on the 2^{nd} order directional derivative that, in GB+AWGN scenarios, fails to correctly detect edges and contours, thus blocking the shock filter's natural time evolution.

By knowing these *a priori* limitations of the classic model, a series of steps towards improving its overall performance were taken over time. Noteworthy results were described in [2], [4] and [8], the edge detector and its robustness being their main focus, somehow neglecting the global GB+AWGN scenario. This generalized scenario was approached in [3] and [5] where the useful signal, affected by both GB and AWGN was part of the problem's statement.

A. Elmoataz et al. (Eds.): ICISP 2010, LNCS 6134, pp. 19–27, 2010.

The starting point of our approach is represented by the work described in [5] that contains a series of innovative ideas at the level of contour detection as well as image-definition domain. Nevertheless, handling both contamination sources at the same time implies a series of compromises either processing quality wise, noise removal wise or edge enhancement wise. In the case of the method described in [5], in order to surmount the inherent classic edge detector's limitations, a new approach was proposed: an approximation of the 2^{nd} order directional derivative given by the imaginary part of the image function. In order to accomplish this, the image definition domain needs to be changed from the real one to the more general domain, the complex one, thus adding a new dimension to the work space. The major improvement brought by this edge detector consists in its robustness to noise, even when dealing with low signal-to-noise ratio (SNR) images. On the other hand, this edge detector presents a noticeable drawback as well, due to the fact that the edge detector will continuously evolve over time, leading to a divergent effect of the filtered result instead of reaching a steady-state solution, as in the case of the classic shock filter.

2 Shock Filter Theory Review

As previously stated, the main limitation of traditional shock filters is the presence of AWGN as contamination source of the useful signal. Since traditional shock filters were initially designed to deal exclusively with GB signal corruption, the more general scenario, GB+AWGN, proves to be too complex for a classic shock filter like the one described in [1]. The GB+AWGN scenario represents a complex perturbation, difficult to filter using traditional methods, requiring either complex processing models or successive filtering for removing each distortion at a time.

The qualitative level of the filtering also depends, to a great extent, on the discretization method used for the mathematical model. An alternative discretization scheme, described in [4], allows the classic shock filter to perform well even in AWGN scenarios, but only for large SNR values, i.e. small AWGN signal corruption.

When dealing with just AWGN perturbations, the usual PDEs framework approach is the use of diffusion filters; this type of filters performs a controlled GB filtering based on the principle of heat dissipation, described in Physics. The controlled GB filtering is behaviorally similar to the GB distortion, hence it can be inferred that the noise removal GB filtering in the AWGN scenario can be approximated to the GB distortion in the GB perturbation scenario. Therefore, in the case of the generalized scenario of GB+AWGN the separate filtering of each distortion is performed with filters opposite in nature, leading to a complex problem. This problem is discussed in [3] and [5], leading to an elegant solution by defining a series of connecting terms between the filtered image and the input image in order to preserve coherence and avoid the filtered image's divergence (absence of a steady-state solution) induced by the opposite nature of the two filtering processes.

The novelty of the idea described in [5] arises from the purpose of the method: to use a shock filter for processing AWGN-corrupted images not just GB-corrupted ones. In order to attain this desideratum the edge detector needs to be rethought, since the classic edge detector is not adequate in handling AWGN-corrupted signals, as

previously stated. The solution given in [5] consists in redefining the definition domain of the image function, from the real one to the complex one. By doing so, the use of the imaginary part of the image function as an edge detector proves to be an elegant and efficient solution in overcoming the classic edge detector's problem.
The general shock filter 1D equation is the following:

$$I_t = -\left|I_x\right| \cdot F(I_{xx}) . \tag{1}$$

With F satisfying the following constraints:

$$\begin{cases} F(0) = 0 . \\ F(s) \cdot sign(s) \geq 0 . \end{cases} \tag{2}$$

By choosing $F(s) = sign(s)$ one obtains the classic shock filter expression:

$$I_t = -sign(I_{xx}) \cdot \left|I_x\right| . \tag{3}$$

When dealing with images, we generally work in a 2D or higher framework. For the 2D case, (3) becomes:

$$I_t = -sign(I_{\eta\eta}) \cdot \left|\nabla I\right| . \tag{4}$$

η represents the gradient vector's direction.

An important role in the discretization of (4) is played by the way in which the gradient norm $|\nabla I|$ is computed, in order to avoid the algorithm's instability caused by the approximation of the 1st order derivatives when computing the gradient vector. A way around this problem is described in [1] where the gradient norm $|\nabla I|$ is computed using a slope limiter *minmod* function in order to minimize the sudden signal variations.

The classic shock filter model from (4) combined with its discretization using the *minmod* function is extremely sensitive to AWGN perturbations, as stated in [1]. The filtering of a GB-corrupted signal with overlaid AWGN or just of an AWGN-corrupted one using the shock filter (4), will amplify the AWGN instead of successfully processing it. If we consider the image function over a continuous domain, the noise amplification can lead to an infinite number of inflexion points, thus resulting in the image function's rapid divergence from a steady-state solution.

Another way to address the AWGN problem is to consider a more complex approach of the shock filter formalism. Such an approach would combine a deblurring method with a noise removal method: for the isotropic regions of the image, a noise removal will take care of the AWGN distortion; as for the anisotropic regions, such as edges and contours, a local, image geometry-driven deblurring will take care of the GB distortion.

Such an approach is presented in [2] and consists in coupling a diffusion filter with a shock filter:

$$I_t = -sign(G_\sigma * I_{\eta\eta}) \cdot \left|\nabla I\right| + cI_{\xi\xi} . \tag{5}$$

σ is the standard deviation of the Gaussian kernel G and c is a positive constant; ξ defines the direction orthogonal to the gradient vector. A more complex mathematical model is described in [3]:

$$I_t = \alpha_r \cdot (h_\tau I_{\eta\eta} + I_{\xi\xi}) - \alpha_e \cdot (1 - h_\tau) \cdot sign(G_\sigma * I_{\eta\eta}) \cdot |\nabla I| . \quad (6)$$

Where: $h_\tau = h_\tau(|G_{\bar{\sigma}} * \nabla I|) = 1 \quad if \ |G_{\bar{\sigma}} * \nabla I| < \tau \quad and \ 0 \ otherwise.$

In order to improve the filtering capacity, [5] firstly suggests changing the sign function F described by (2), to allow taking into account not only the 2nd order derivative's direction but also its magnitude. This way the inflexion points (the regions close to contours/edges where the 2nd order derivative has a higher magnitude) will not have equal weights, which translates into a higher deblurring speed near edges and contours than in the isotropic regions of the image. The new sign function is expressed as follows:

$$F(s) = \frac{2}{\pi} \arctan(as) . \quad (7)$$

In (7) a is the parameter that controls the steepness of the 2nd order derivative's slope near 0.

Finally, [5] proposes a complex shock filter model that employs the sign function (7), having the following expression:

$$I_t = -\frac{2}{\pi} \arctan(a \cdot \mathrm{Im}(I/\theta)) \cdot |\nabla I| + \lambda I_{\eta\eta} + \tilde{\lambda} I_{\xi\xi} . \quad (8)$$

Where $\lambda = re^{i\theta}$ is a complex scalar, $\tilde{\lambda}$ is a real scalar and $\theta \in (-\pi/2, \pi/2)$.

For small values of θ ($\theta \to 0$), the imaginary part can be regarded as a smoothed 2nd order derivative of the initial signal factored by θ and the time t, as it was mathematically proven in [6]. The implementation of (8) is done by the same standard discrete approximations used in [1], except that all computations are performed in the complex domain.

3 The Hybrid Shock Filter Model

Although the complex shock filter described in [5] proves to be a viable alternative to the classic one in circumventing the noise problem in the generalized scenario of GB+AWGN interference, it presents at the same time a series of shortcomings, the most important of them being its numerical implementation, which becomes unstable after a sufficiently large number of iterations. This translates into the method's dependency on the human supervised control, the algorithm's stopping criterion being tied to its input parameters and sensitive to the nature of the input image.

These shortcomings along with the ones presented by the classic model represent the premises of our hybrid shock filter model. Our goal is to combine the advantages of both models without preserving any of their disadvantages. So far our hybrid model solves the inability to efficiently process AWGN of the classic shock filter as

well as the divergent character of the complex one, thus resulting a shock filter capable of image enhancement in GB+AWGN scenarios that is both efficient and stable. Another advantage of this method resides in its modularity, allowing the use of multiple sets of functions, useful in the filter's behavioral analysis over a large variety of input images.

The mathematical expression of the hybrid shock filter is the following:

$$\begin{aligned}\mathrm{Re}(I_t) &= -\frac{2}{\pi}\arctan(a\cdot \mathrm{Im}(I)/\theta)\cdot f_1\cdot|\nabla I| - sign(\mathrm{Re}(I_{\eta\eta}))\cdot f_2\cdot|\nabla I| \\ &\quad + f_1\cdot(\mathrm{Re}(\lambda)\cdot \mathrm{Re}(I_{\eta\eta}) - \mathrm{Im}(\lambda)\cdot \mathrm{Im}(I_{\eta\eta}) + \tilde{\lambda}\,\mathrm{Re}(I_{\xi\xi}))\,. \\ \mathrm{Im}(I_t) &= \mathrm{Im}(\lambda)\cdot \mathrm{Re}(I_{\eta\eta}) - \mathrm{Re}(\lambda)\cdot \mathrm{Im}(I_{\eta\eta}) + \tilde{\lambda}\,\mathrm{Im}(I_{\xi\xi})\,.\end{aligned} \tag{9}$$

The parameters of (9) have the following significance:

- a is the parameter that controls the slope of the edge detector's sign function (*arctan*).
- $\theta\in(-\pi/2,\pi/2)$ is an input parameter. When $\theta\to 0$, $\mathrm{Im}(I)/\theta$ can be approximated to the 2nd order directional derivative of the image function I.
- $|\nabla I|$ represents the gradient norm of function I computed using the *minmod* function as defined in [1].
- $\lambda = re^{i\theta}$ is a complex scalar parameter, computed as a function of θ.
- $\tilde{\lambda}$ is a real scalar input parameter.
- f_1 and f_2 are two complementary functions that represent the core of the hybrid shock filter formulation (9). Their purpose is to control the nature of the hybrid shock filter, i.e. to control the transition rate of the filter's behavior from an exclusively complex one to an exclusively real one. These functions are defined as follows:

$$f_1(T_{I1},T_{S1}) = \begin{cases} 1, & i < T_{I1} \\ 1-\dfrac{i-T_{I1}}{T_{S1}-T_{I1}}, & T_{I1}\le i < T_{S1}, \\ 0, & i \ge T_{S1} \end{cases} \quad \begin{array}{l} i = 0\ldots N-1, \\ T_{I1},T_{S1}\in(0;N-1) \end{array}$$

$$f_2(T_{I2},T_{S2}) = \begin{cases} 0, & i < T_{I2} \\ \dfrac{i-T_{I2}}{T_{S2}-T_{I2}}, & T_{I2}\le i < T_{S2}, \\ 1, & i \ge T_{S2} \end{cases} \quad \begin{array}{l} i = 0\ldots N-1, \\ T_{I2},T_{S2}\in(0;N-1) \end{array} \tag{10}$$

N represents the number of iterations, correlated with the mathematical model's time parameter t ($t = dt\cdot N$). $T_{I1},T_{S1},T_{I2},T_{S2}$ are threshold parameters used to define the complementary behavior of f_1 and f_2; $f_1,f_2: [0;N\text{-}1]\to[0;1]$ as exemplified in Fig. 1:

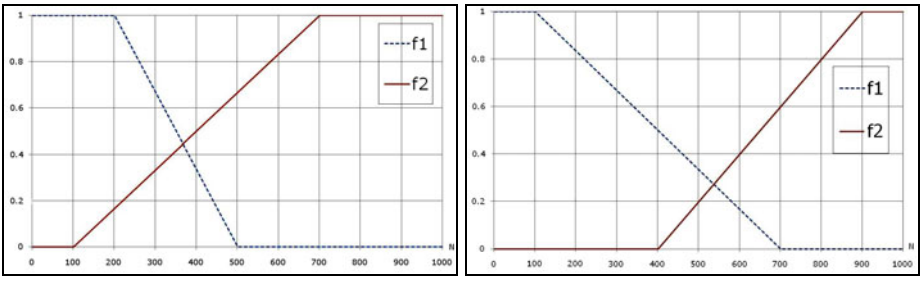

Fig. 1. Graphical representation of f_1 and f_2 (10) for: $T_{I1} = 200$; $T_{S1} = 500$ / $T_{I2} = 100$; $T_{S2} = 700$ - *left* and $T_{I1} = 100$; $T_{S1} = 700$ / $T_{I2} = 400$; $T_{S2} = 900$ - *right*

The hybrid shock filter has a combined behavior, weighted by its control functions f_1 and f_2 that could be summarized as follows:

- When f_1=1 and f_2=0 the filter behaves exclusively as a complex shock filter (described in [5]). This behavior is required in order to effectively deal with the AWGN perturbation that can be approached using the complex shock filter paradigm. Thus, the hybrid shock filter relies on its edge detector (imaginary part of the image function *I*) in correctly detecting edges and contours in GB+AWGN conditions.
- Following its time evolution, after a certain number of iterations the AWGN will be filtered enough to use the classic shock filter component of the hybrid shock filter. This is the case when $f_1 \in [0;1)$ and $f_2 \in [0;1)$, translating into a simultaneous evolution of both hybrid shock filter's components.
- Finally, at the end of the filtering process, f_1=0 and f_2=1 allowing the hybrid shock filter to properly act as an edge enhancement filter (filtering the GB perturbation) through its classic shock filter component.

4 Experimental Results

In order to carry out the performance analysis, as well as the comparative study of the hybrid shock filter, we first need to define the experimental setting: a test image distorted with a GB+AWGN-type distortion (Fig. 2b) with the following parameters: GB with $\sigma = 5$ and AWGN of amplitude $A = 30$. The comparative analysis between the three types of shock filters (classic, complex and hybrid respectively) will be performed using as an objective quality assessor the Root-Mean-Square-Error (RMSE) measurement and as a subjective quality assessor the visual comparison between the unaltered test image and the filtered results. Fig. 2 represents the experimental setting as well as the filtered results.

For the above test scenario: the test parameters were the following: $\theta = 0.00001$, $\tilde{\lambda} = 0.5$, a = 0.5, $|\lambda| = 0.5$ $dt = 0.1$ and $N = 1000$ leading to a theoretical evolution time of $t = 100$ seconds. It needs to be emphasized that the classic shock filter only uses two parameters (*dt* and *N*) while the complex and hybrid shock filters use the

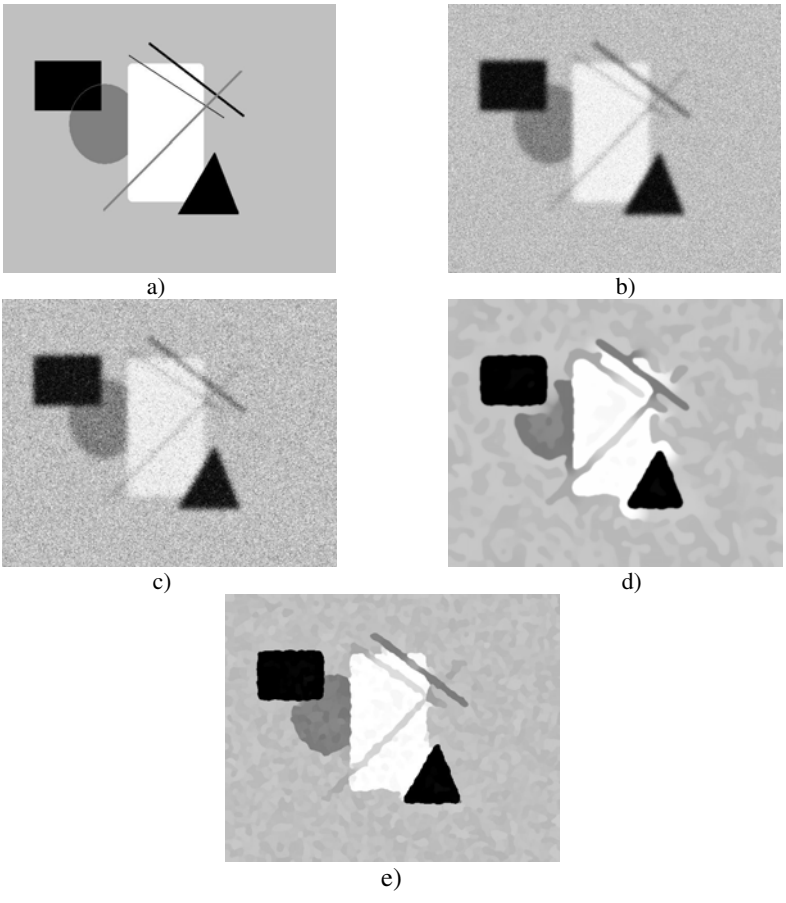

Fig. 2. Experimental setting: a) Original test image; b) Distorted test image; c) Classic shock filter result; d) Complex shock filter result; e) Hybrid shock filter result

same parameters with the remark that for the hybrid shock filter the function set (10) was used with the following parameters: T_{I1} =300;T_{S1} = 350 / T_{I2} = 320;T_{S2} = 900.

Fig. 3 represents the RMSE/time evolution of the three filters, according to the experimental setting described by Fig. 2. The RMSE measurement was performed between the unaltered image (Fig. 2a) and each of the three filtered results (Fig. 2c-2e). As it can be noted, the hybrid shock filter possesses the advantages of both the classic shock filter (stable time evolution, steady-state solution) and the complex one (efficient AWGN filtering as well as GB deblurring). Since any output image is considered to be information and according to the definition of information, it represents an entity about which we do not possess any prior knowledge, it is impossible to *a priori* know the minimum value of the RMSE obtained by filtering. Thus, the complex shock filter lacks the ability of maintaining a stable behavior (that leads to a steady-state solution) long enough to ensure that its time evolution has reached the minimum RMSE value before diverging.

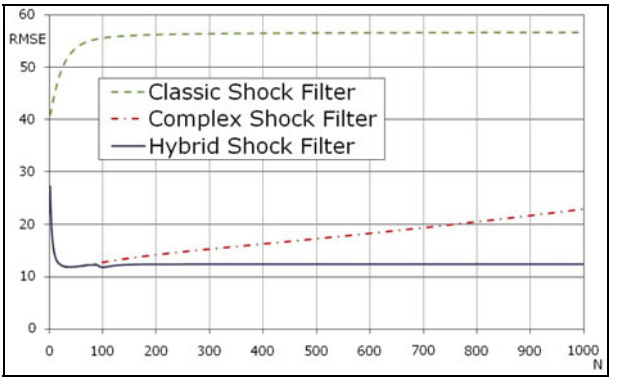

Fig. 3. RMSE comparison between the three shock filters

5 Conclusions

While still a work in progress, the hybrid shock filter model has proven so far a step forward in shock filter theory, turning out to be a viable alternative to the classic methods in both GB, AWGN and GB+AWGN scenarios. The mathematical model allows further improvements, from minor tweaks in control function definition to increasing the filtering capacity as well as the convergence speed towards a steady-state RMSE value.

The experimental results and comparative analysis were promising, establishing the premises for future shock filter theory paradigms.

Acknowledgment. This work was supported by CNCSIS-UEFISCSU, project number PNII-IDEI code 908/2007.

References

1. Osher, S., Rudin, L.: Feature-oriented Image Enhancement Using Shock Filters. SIAM J. on Num. Anal. 27, 919–940 (1990)
2. Alvarez, L., Mazorra, L.: Signal and Image restoration Using Shock Filters and Anisotropic Diffusion. SIAM J. on Num. Anal. 31, 590–605 (1994)
3. Kornprobst, P., Deriche, R., Aubert, G.: Image Coupling, Restoration and Enhancement via PDEs. In: International Conference on Image Processing (ICIP) Proceedings, vol. 2, pp. 458–461 (1997)
4. Remaki, L., Cheriet, M.: Numerical Schemes of Shock Filter Models for Image Enhancement and Restoration. J. of Math. Imag. And Vis. 18, 129–143 (2003)
5. Gilboa, G., Sochen, N.A., Zeevi, Y.Y.: Regularized Shock Filters and Complex Diffusion. In: Heyden, A., Sparr, G., Nielsen, M., Johansen, P. (eds.) ECCV 2002. LNCS, vol. 2350, pp. 399–413. Springer, Heidelberg (2002)
6. Gilboa, G., Zeevi, Y.Y., Sochen, N.A.: Complex Diffusion Processes for Image Filtering. In: Kerckhove, M. (ed.) Scale-Space 2001. LNCS, vol. 2106, pp. 299–307. Springer, Heidelberg (2001)

7. Gilboa, G.: Super-resolution Algorithms Based on Inverse Diffusion-type Processes. PhD Thesis, Technion-Israel Institute of Technology, Haifa (2004)
8. Weickert, J.: Coherence-Enhancing Shock Filters. In: Michaelis, B., Krell, G. (eds.) DAGM 2003. LNCS, vol. 2781, pp. 1–8. Springer, Heidelberg (2003)
9. Tschumperle, D., Deriche, R.: Constrained and Unconstrained PDEs for Vector Image Restoration. In: 12th Scandinavian Conference on Image Analysis, Norway, pp. 153–160 (2001)
10. Buades, A., Coll, B., Morel, J.M.: Image Enhancement by Non-local Reverse Heat Equation (Preprint CMLA 2006-22) (2006)
11. Buades, A., Coll, B., Morel, J.M.: The Staircasing Effect in Neighborhood Filters and its Solution. IEEE Transactions on Image Processing 15(6), 1499–1505 (2006)
12. Rudin, L.: Images, Numerical Analysis of Singularities and Shock Filters. PhD Thesis, California Institute of Technology, Pasadena CA (1987)
13. Barash, D.: One-step Deblurring and Denoising Color Images Using Partial Differential Equations. HP Laboratories, Israel (2001)
14. Welk, M., Theis, D., Borx, T., Weickert, J.: PDE-based Deconvolution with Forward-Backward Diffusivities and Diffusion Tensors. In: Kimmel, R., Sochen, N.A., Weickert, J. (eds.) Scale-Space 2005. LNCS, vol. 3459, pp. 585–597. Springer, Heidelberg (2005)
15. Bettahar, S., Stambouli, A.B.: Shock Filter Coupled to Curvature Diffusion for Image Denoising and Sharpening. Imag. and Vis. Comp. 26(11), 1481–1489 (2008)